On Thermal Energy Storage Capacity for CSP Plant in South Africa

Hoffmann[a], J.E. and Madaly[b], K.

Received 20 January 2015, in revised form 25 May 2015 and accepted 9 October 2015

We have demonstrated that the minimum levelized cost of electricity from a molten salt central receiver plant with a given heliostat field configuration is driven by a single independent variable, namely the thermal energy storage capacity in hours of full time turbine operation. In our model, the solar multiple, number of heliostats and receiver heat flux all depend on the thermal energy storage. The lowest levelized cost corresponds to 14 hours thermal energy storage. The levelized cost for a 100 MW$_e$ net plant in Upington, South Africa is expected to come in between 15 ¢/kWh$_e$ and 20 ¢/kWh$_e$.

Additional keywords: Central receiver, molten salt, levelized cost

1 Introduction

South Africa, and specifically the arid north western part of it, is blessed with an exceptional solar resource. The long term annual average solar irradiation for Upington[1], South Africa is 2 816 kWh/m^2. However, due to a cheap and abundant coal supply, electricity generation in the country has been derived from coal for the past century. Since 2010, renewable energy has been considered in the country's energy mix. The Kaxu-1 (100 MW parabolic trough), Khi-1 (50 MW central receiver, direct steam generation) and Bokpoort (50 MW parabolic trough with 9 hours thermal energy storage) plants are currently under construction, with the Kaxu plant scheduled to come on-line in February 2015 and Bokpoort in December 2015. A contract has been awarded for the construction of another 100 MW parabolic trough plant at the Kaxu site. Due to water scarcity in South Africa in general, and its north western parts in particular, all plants are dry cooled.

The South African state-owned utility ESKOM intends to build a 100 MW plant near Upington. The proposed plant will have molten salt as heat transfer fluid, and should include thermal energy storage. Madaly[2] did a techno-economic optimization for this plant. In the current study, we have refined some technical aspects of our model. We also reduced the number of independent variables in our analysis, and updated the financial figures where appropriate. Cost estimates for South African plant currently under construction is treated as confidential information, and we had to rely on international reports[3, 4, 5] for our estimates.

a. Dept. of Mechanical and Mechatronic Engineering, Stellenbosch University, Private Bag X1, Matieland, 7602, South Africa (hoffmaj@sun.ac.za)
b. Plant Engineering Dept., Koeberg Nuclear Power Station, West Coast Road, Melkbosstrand, South Africa.

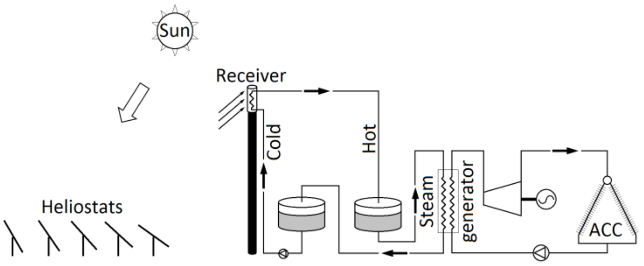

Figure 1: Process description for central receiver plant with thermal energy storage.

Figure 1 illustrates the processes in a central receiver solar power plant with storage. Sun tracking mirrors (heliostats) focus the sun's energy onto the receiver, where solar radiation is transferred to the molten salt as thermal energy. The salt leaving the receiver is collected in the hot salt tank. Molten salt is extracted from the hot salt tank, and passed through the steam generator, where its heat is transferred to the high pressure water and steam. The steam drives the steam turbine, which in its turn powers the generator. Low pressure steam is condensed in the air cooled condenser, pumped to the desired pressure from where it repeats the cycle. Salt leaving the steam generator is collected in the cold salt tank, from where it is pumped back to the receiver.

Thermal energy storage increases the plant's capacity factor, and as a result tends to reduce the levelized cost of electricity. It could also potentially increase the plant's profitability, as the South African electricity tariff is structured such that a premium of up to four times the off-peak price is earned during peak times, typically early evening[6]. The Gemasolar Thermosolar Plant (20 MW, 15 hours thermal energy storage) in Spain is the world's first commercial molten salt central receiver plant with thermal energy storage. It has proven that the technology is viable on a commercial scale[7] with capacity factors in excess of 70%. Gemasolar has demonstrated full load electricity production over a 24 hour period for 36 consecutive days.

2 Model Description

2.1 Heliostat field

Direct normal irradiation (DNI), air temperature and wind speed were measured from 1994 – 2000 at Upington[1], and hourly averaged values were available for all three variables for a typical meteorological year. The DNI values for the first seven days of the typical meteorological year from[1] are given in figure 2. Sun angles were calculated from Duffie and Beckman[8]. Plant transients were modelled as if the plant is running through successive hourly steady state operating conditions, with unique DNI and ambient conditions for every hour. The DNI, air temperature and wind speed are kept constant at their average values during each hour. We assumed a step change with no delay from one hourly average to the next. Solar energy harvesting starts immediately if the

DNI exceeds zero. No threshold was set for the minimum DNI required before the heliostat field and molten salt pumps are activated. The power blocks draws energy from the thermal energy storage, and it should not be subjected to fast transients.

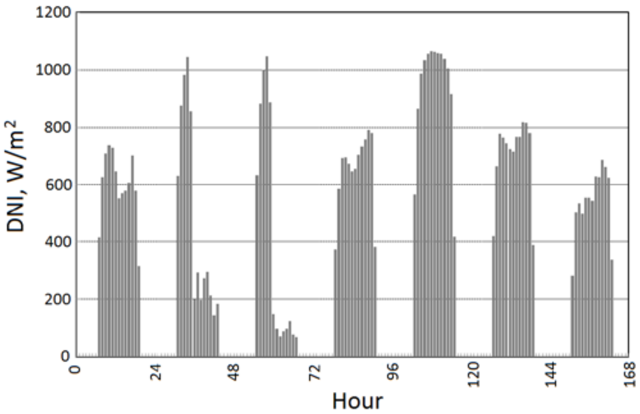

Figure 2: Hourly DNI values for the first seven days of the typical meteorological year, Upington.

For a surround field, the optical efficiency (cosine, blocking and shading efficiencies) of the heliostat field is dominated by the zenith angle[9]. Here, despite the site being selected, the actual heliostat field lay-out is as yet not determined, and we have adopted Gauché et al's[9] correlation for the Gemasolar plant. We have assumed constants for reflection, fouling, attenuation and spillage losses[10]. The maintenance schedule comprise of an 8 day annual outage, and a 60 day outage every 10 years[10]. We have rounded this up to include on-line individual heliostat maintenance activities to a 96 % plant availability.

2.2 Receiver

We have assumed an external receiver, with a 60 % $NaNO_3$ by weight / 40 % KNO_3 by weight molten salt flowing vertically through circular tubes. For this salt mixture, crystallization starts at 240 °C, whilst the salt will start to decompose[11] at temperatures above 600 °C. Only the total collected energy from the heliostat field is calculated, and no provision is made for the circumferential variation of the incoming heat flux, that will change throughout the day. An energy balance for the receiver yields the heat transfer to the salt, $\dot{Q}_{salt}$:

$$\alpha\dot{Q}_{opt} = \sigma\varepsilon FA(\bar{T}_m^4 - T_a^4) + UA(T_s - T_a) + \dot{Q}_{salt} \qquad (1)$$

with $\dot{Q}_{opt}$ the heat received from the optical field, A the surface area of the receiver, F is the radiation shape factor, α the absorptivity of the receiver surface, ε its emissivity and σ the Stefan-Boltzmann constant. The overall heat transfer coefficient is U ($U \approx h$, with h the air side convective heat transfer coefficient), whilst T_s and T_a are the salt and air temperatures respectively. Finally, $\bar{T}_m$ is the mean radiation temperature, that differs from the arithmetic mean receiver surface temperature.

The receiver heat flux q''_{max} is limited[4] to 700 kW_t/m^2, and its assumed aspect ratio (L/D) is 1.6, allowing us to calculate its height, L and diameter D.

The receiver loses radiation to the ground, air and surrounding structures. It is assumed that these are all at the ambient air temperature. Since $T_a \ll \bar{T}_m$, the impact of this assumption should be insignificant. Furthermore, it is assumed that the radiation shape factor is 1 as the receiver is fully enclosed by its environment. The radiation loss is found from integration over the receiver surface

$$\begin{aligned}\dot{Q}_{rad} &= \sigma\varepsilon\int_0^L [T^4(\xi) - T_a^4]\pi D\, d\xi \\ &= \pi D\sigma\varepsilon\int_0^L T^4(\xi)d\xi - \sigma\varepsilon\pi DLT_a^4 \\ &= \sigma\varepsilon\pi DL(\bar{T}_m^4 - T_a^4)\end{aligned} \qquad (2)$$

For a linear salt temperature distribution in the receiver (once through salt flow), the mean receiver surface temperature is given by

$$\begin{aligned}\bar{T}_m^4 &= \int_0^L T^4(\xi)d\xi \\ &= \frac{T_{max}^4 + T_{max}^3T_{min} + T_{max}^2T_{min}^2 + T_{max}T_{min}^3 + T_{min}^4}{5}\end{aligned} \qquad (3)$$

with

$$T_{max} = T_{so} + \frac{2q''_{max}\, D_o\, log(D_o/D_i)}{k_w}$$

and

$$T_{min} = T_{si} + \frac{2q''_{max}\, D_o\, log(D_o/D_i)}{k_w}$$

In the equation above, T_{so} and T_{si} are the salt outlet and inlet temperatures respectively, D_i and D_o the receiver tube inner and outer diameters, k_w the thermal conductivity of the tube material, and q''_{max} the incoming heat flux at the receiver surface. The heat transfer coefficient on the inside of the tube is large.

Convection losses comprise of natural and forced (wind driven) convection. Available correlations[12] for mixed convection across vertical cylinders do not span the Rayleigh numbers encountered in concentrated solar power. The average heat transfer coefficient is estimated from

$$h = \sqrt{h_{nc}^2 + h_{fc}^2} \qquad (4)$$

In this form, the heat transfer coefficient is dependent on the magnitude of the mixed velocity across the receiver, and it will recover both limiting cases for wind driven convection when $h_{nc} = 0$ and natural convection for which $h_{fc} = 0$.

The Nusselt number, Nu_{nc} for natural convection is calculated from the Rayleigh number Ra[13]

$$Nu_{nc} = \frac{h_{nc}D}{k_a} = 0.1\, Ra^{1/3} \qquad (5)$$

with k_a the thermal conductivity of air. Air properties are evaluated at the mean film temperature. The mean receiver surface temperature is given by

$$T_{surf} \approx \frac{T_{so}+T_{si}}{2} + \frac{2q''_{max}D_o\, log(D_o/D_i)}{k_w} \qquad (6)$$

The receiver is approximated as a cylinder, and the forced convection heat transfer coefficient for flow across a circular cylinder is given by Zukauskas (in Çengel and Ghajar[13])

$$Nu_{fc} = \frac{h_{fc}D}{k_a} = 0.027Re^{0.805}Pr^{0.333} \qquad (7)$$

with Re and Pr the Reynolds and Prandtl numbers respectively. Air properties are once again evaluated at the mean film temperature. The actual shape of the wind profile depends on the atmospheric stability[14], but for convenience the wind speed at the receiver height is evaluated from the 1/7th law for the boundary layer over flat surface:

$$V(z) = V_{10}\left(\frac{z}{10}\right)^{1/7} \tag{8}$$

The wind speed at 10 m above ground level is included in the meteorological data for the given site.

2.3 Thermal Energy Storage

It is assumed that thermal energy storage loss is restricted to the side wall of the tank, and only up to the salt level inside the tank. Hence there is a linear relationship between heat loss from the tank and the salt inventory stored inside the tank. We assume that the overall heat transfer coefficient is constant ($U \approx 6$ W/°C m^2 resulting in a loss of about 1.5 % of stored energy per day from a fully charged tank, as suggested by Sioshansi and Denholm[15]. Hence

$$\dot{Q}_{tl} = \pi D H_{salt} U(T_{salt} - T_a) \tag{9}$$

A detailed estimate of the heat losses in a storage tank is offered by Pérez-Segarra et al[16]. If the storage runs out, the turbine will only restart if the receiver heat flux is sufficient for full load operation. This will partially offset the thermal lag of the plant.

2.4 Steam Generator

The steam generator links the power block and thermal energy storage. Indirect energy feed is from the hot salt tank. The steam generator consists of a preheater, evaporator, and a superheater and reheater in parallel. The salt exit temperature from the latter components is assumed equal. With this assumption, the split in salt flow between the reheater and superheater can be determined.

Behbahani-nia, Sayadi and Soleymani[17] optimized the pinch point for a heat recovery boiler, and found that the thermodynamically optimized pinch point, ΔT_{pinch} (see figure 3) is about 5 °C. Although their work is not directly applicable to molten salt steam generators, the pinch point is set to 5 °C.

With the hot salt temperature fixed to 565 °C, the salt flow rate is found from an energy balance on the steam generator, from the evaporator inlet to the superheater and reheater outlets.

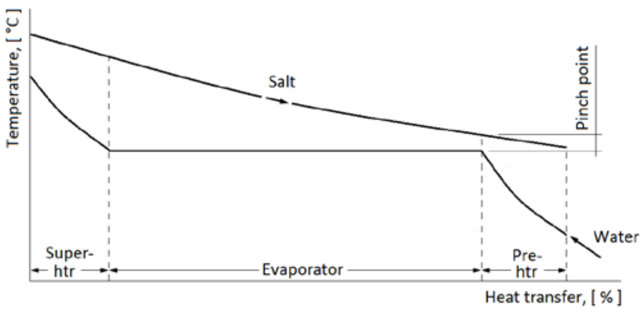

Figure 3: Water and salt temperature profiles in steam generator.

$$\dot{m}_{salt}\bar{C}_{p,salt}\left[T_{salt,in} - \left(T_{sat} + \Delta T_{pinch}\right)\right] = \dot{m}_{live}(h_{SH} - h_{FW}) + \dot{m}_{RH}\Delta h_{RH} \tag{10}$$

with $\dot{m}_{salt}$ the salt mass flow rate, $\bar{C}_{p,salt}$ the specific heat of the salt at the mean salt temperature, T_{sat} the saturation temperature of water/steam at the live steam pressure, $\dot{m}_{live}$ the steam flow through the high pressure turbine, $\dot{m}_{RH}$ the steam flow through the reheater, h_{SH} the enthalpy of the steam leaving the superheater, h_{FW} the enthalpy of the saturated feedwater entering the evaporator and Δh_{RH} the enthalpy increase over the reheater. Once the salt flow rate is known, the cold salt temperature is determined uniquely. The cold salt temperature is not allowed to drop below 260 °C. However, with the pinch point and live steam pressure set at 5 °C and 130 bar respectively, the cold salt temperature varies in a narrow band around 273 °C.

2.5 Power block

The power block assumes a Rankine cycle with single reheat, and is loosely based on the Siemens SST-800 series turbines[18]. For this turbine, the live steam pressure and temperature are 130 bar and 540 °C respectively. It is assumed that the characteristic time of the power block is small relative to temporal changes in DNI, allowing the power block to be modelled as successive hourly steady states. The Microsoft Excel add-in X Steam[19] was used to calculate the thermodynamic properties of water and steam.

The thermal efficiency of a Rankine cycle with superheat will increase for increasing life steam pressure and temperature[20]. This will reduce the steam consumption, resulting in a smaller optical field and thermal storage tanks. These trends were confirmed by Madaly and Hoffmann[2], hence the live steam conditions were fixed at the maximum rating of the turbine.

Reheat pressure is assumed to be ¼ of the life steam pressure. The isentropic efficiency of the high and low pressure turbines are 82 and 90 % respectively[18]. Waste heat is rejected to the atmosphere in a forced draft air cooled condenser. Pretorius and Du Preez[21] suggest that the condensing temperature is 25 °C – 30 °C above the ambient dry bulb temperature, and that the temperature difference varies slightly with ambient temperature. They showed that the initial temperature difference has a minimum at the design point. Here, we assumed that initial temperature difference at the air cooled condenser is a constant 25 °C.

The plant is fitted with six feedwater heaters, as shown in figure 4, and it is assumed that the steam extraction points at the low pressure turbine are at equal increments of saturation temperature[20]. Increasing the number of feedwater heaters will increase the thermal efficiency of the plant, albeit at diminished returns for a higher number of feedwater heaters[20]. A recent study by Söylemez[22] on a 1 MW fossil fuel fired plant suggests that the economic optimum number of feed heaters might be lower. Our cost model is based on National Renewable Energy Laboratory data[3] for a plant with six feedwater heaters, a number we have adopted for this study. We further assume a temperature difference of 5 °C between the water leaving the feedwater heater, and the condensing steam. The steam exits the feedwater heater as saturated liquid and is dumped directly into the air cooled condenser sump (low pressure heaters) or deaerator (high pressure heaters). The final feedwater heater is supplied from the cold reheat steam, and its saturation temperature determines the maximum feedwater temperature. Our earlier work[2] allowed for steam extraction from the high pressure turbine casing. With these assumptions, one can calculate the extraction rates for each feedwater heater. Pressure drop across the feedwater heaters is ignored.

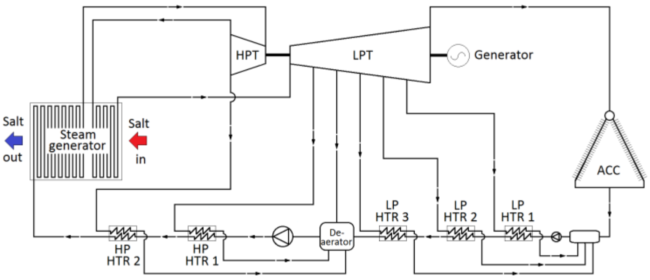

Figure 4: Thermodynamic cycle for central receiver plant with thermal energy storage.

We have validated our power block model against simulation results for the same plant on the commercial steam plant design and simulation code Steam Pro[23].

Parasitic load (salt pumps, trace heating, air cooled condenser fans, etc.) is estimated at 10 % of the gross power generated[24].

2.6 Solar Multiple

The plant's design point is for noon on the vernal equinox (20 March) in the typical meteorological year. A solar multiple of 1 means that the optical field is sized such that the plant is capable of achieving full load at the design point, as shown in figure 5. For a solar multiple greater than 1, the energy harvested from the solar field exceeds the demand of the power block some of the time. This means that some heliostats need to defocus on a plant without thermal energy storage. In the case of a plant equipped with energy storage, the excess energy is collected in the hot salt tank, to be used at a later stage, typically during the night or at times of inclement weather. Madaly[25] assumed that the solar multiple is independent of the storage time. Here, the solar multiple is a function of thermal energy storage. It is adjusted to allow full load operation at the design thermal efficiency for the entire storage time.

The number of heliostats required is calculated to match the turbine's heat consumption at the design point, and then multiplied by the solar multiple. Although the number of heliostats scales linearly with the thermal energy storage capacity, the additional capital cost of the heliostats is offset by extending electricity generation into the night.

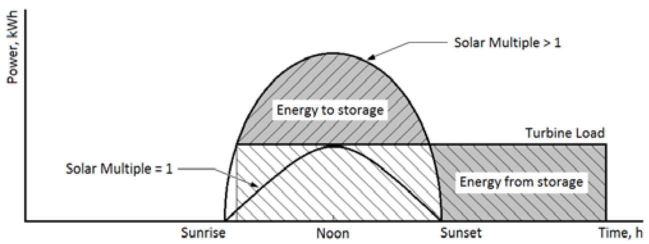

Figure 5: Conceptual relationship between solar multiple and thermal energy storage.

2.7 Calculation of the Levelized Cost of Electricity (LCOE)

ESKOM currently pays 7.65 % interest[26] on their loans, but can expect a rate increase in future as both ESKOM and South Africa have been downgraded by credit rating organizations. Both the interest rate and inflation rate is subject to change over time, requiring projected future rates. The South African economist Dawie Roodt suggested on radio that ESKOM should be able to raise a loan at an interest rate of 9 % with government guarantees. For this study, we have adopted flat rates over the life of the plant. It is assumed that a 100 % loan is obtained at an interest rate of $i = 9$ % with loan duration of 27 years. The inflation rate corresponds to the upper limit of the South African reserve Bank's inflation target, and is equal to $r = 6$ %. The rand dollar exchange rate at the time of writing is ≈ R/$=11. The LCOE is given by

$$LCOE = \frac{\sum_{j=1}^{N}(I_j + M_j)/(1+r)^j}{\sum_{j=1}^{N} W_{e,j}/(1+r)^j} \quad (11)$$

with M_j the annual operating and maintenance cost, and W_e the net power generation. The annual financing cost is given by

$$I_j = \frac{iI_0}{1-(i+1)^{-N}} \quad (12)$$

where I_0 is the amount of the initial loan, i the interest on the loan and N the loan period. The cost breakdown for the plant is shown in table 1. We have assumed that the total loan amount is taken out up front, but the plant will only produce electricity two years after construction has started. We also ignored the salvage value of the plant at the end of its operating life.

Table 1: Cost estimates for various plant components for central receiver plant.

	Max	Min
Engineering, Procurement and Project Management as % of fixed cost	25	11
Land* ($/ha)[27]	275	145
Site Improvement ($/m^2)	20	15
Solar Field ($/m^2)	200	180
Tower and Receiver ($/kW$_t$)	200	142
Thermal Energy Storage ($/kWh$_t$)	35.5	30
Power block, dry cooled ($/kW$_e$)	1200	1000
Balance of plant, including steam generator ($/kW$_e$)	365	350
Operating and Maintenance:		
Fixed Cost ($/kW$_e$.yr)	70	65
Variable Cost ($/MWh$_e$)	4	3

* The typical farm size for district is 6 000 ha[27].

3 Discussion of Results

Madaly[25] optimized the plant for six independent parameters, the number of feedwater heaters, live steam pressure, feedwater inlet temperature, cold salt temperature, solar multiple and storage time. No detailed cost figures are available for individual feedheaters. From thermo-dynamics[20] it is clear that the plant's thermal efficiency will increase with the number of feedheaters, but that the rate of increase will drop as the number of feedheaters increase. In modern (coal fired) power plant, the number of feedheaters is limited to five or six. The final feedwater temperature is determined by the saturation temperature of the cold reheat steam. Cold salt temperature depends on the pinch point in the steam generator. Lowering the hot salt and steam temperatures may reduce component prices, but once again, no firm costing were available. Hence, the maximum live steam pressure and hot salt temperature were adopted, as it would result in the highest thermal efficiency. It has been shown that the solar multiple is directly linked to the storage time. Consequently, thermal energy storage is the only independent variable left in our model. We have analysed the levelized cost of electricity for two cases. For the first case, we have taken the highest cost listed in Turchi and Heath[3] for all plant items, and in the second, the lowest. The results are presented in figure 6.

A quadratic function fits our data with a correlation coefficient of 0.998. The minimum levelized cost corresponds to the minima of the quadratic function. Figure 6 also shows that the capacity factor is approaching an asymptotic value for large storage times, indicating that the plant is running 24 hours most of the time. Increasing the storage further basically adds to the cost with little or no increase in the electricity output.

In both cases, the levelized cost of electricity has a minimum at 14.3 hours, with the levelized cost be between R 1.68/kWh ($ 0.15/kWh) and R 2.19/kWh ($ 0.20 $/kWh). The deviation from Madaly's earlier work is due to changes in the exchange rate. The current model has a slightly lower overall efficiency, as it predicts higher radiation and convection losses at the receiver. Furthermore, we increased the condenser temperature, and changed the configuration of the feedwater heaters.

Our results show reasonable agreement with recent studies. Ausburger[28] used a multiple objective optimizer to analyse the Gemasolar plant. A total of eight design variables, including the solar field, were varied simultaneously to maximize solar field efficiency and minimize levelized cost of electricity. The receiver heat flux was constrained to 1 500 W/m^2, about double that of our model. Ausburger shows that it is theoretically possible to reduce the levelized cost of electricity for Gemasolar from $0.24/kWh to $0.15/kWh. Hence, our outlook for Upington with its higher solar resource is pessimistic compared to Ausburger.

Avila-Marin, Fernandez-Reche and Tellez[29] analysed a 500 MW_t plant at Carnavon, South Africa. They gave values for relative levelized cost of electricity, that is not directly comparable with our results. However, they did mention that the optimum thermal storage is 14 – 16 hours. Turchi and Heath[3] used NREL's System Adviser Model[30] and predicted an LCOE of $0.14 – $0.15 kWh.

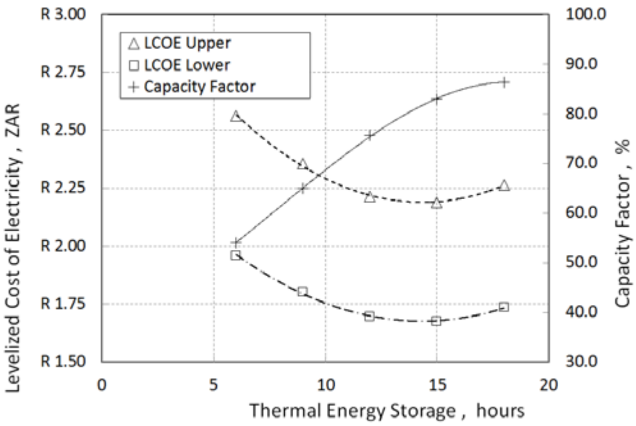

Figure 6: Levelized cost of electricity for central receiver plant near Upington, South Africa.

The levelized cost of electricity for a supercritical coal plant is R0.80/kWh ($0.07/kWh)[31]. This number may increase significantly, as ESKOM faced a 36 % increase in the cost of primary energy (or a 53 % increase[32] in the price of coal) between March 2012 and March 2013. It is not expected that CSP will be price competitive with supercritical coal in the near future. However, rolling out CSP on a larger scale should result in cost reductions from learning rates and economies of scale. CSP can become a key player in the South African energy mix within the next two decades.

4 Conclusion

Concentrated solar power has been identified as a primary long term method of generating electricity in South Africa. However, the technology is new to South Africa, with the first three plants scheduled to come on line in 2015. As yet, no costing data is available for the construction and operation of such plant in South Africa. Published cost estimates vary significantly, prompting us to report on an optimistic versus a pessimistic cost scenario. Land prices were adjusted for the South African market. Specialized labour and material requirements will dictate that the first few plants will rely heavily on imports until sufficient knowledge transfer has taken place to localize plant construction. If renewable energy is to become price competitive in the South African energy market, dominated by coal fired power stations, careful consideration should be given to optimal plant configuration.

We derived a techno-economic model of a 100 MW_e central receiver plant with a two-tank molten salt thermal energy storage. All major plant components are included, and their modelling is based on simple thermodynamic concepts. Our model has been validated against more sophisticated methods on component level. We exploited inter-dependencies between parameters to reduce Madaly's[25] original six independent design variables to one, namely the thermal energy storage capacity in hours of full time plant operation. This allows us to optimize the plant configuration, based upon the integrated plant performance as successive hourly steady states using DNI values for a typical meteorological year almost instantaneously.

Our model predicted the optimum storage capacity to be 14 hours, corresponding to a levelized cost of electricity of R1.68/kWh for the optimistic scenario, and R2.19/kWh for the pessimistic scenario. At present, this is about double the levelized cost of electricity derived from coal in South Africa. Recent steep increases in the cost of primary energy for coal fired power stations[32], and the expected reduction in the LCOE associated with the large scale roll-out of concentrated solar power should narrow the gap in the future.

5 Acknowledgement

This project was supported by a grant from the Eskom Power Plant Engineering Institute (EPPEI).

References

1. *Suri M*, Site assessment of solar resource, Upington Solar Park, Northern Cape Province, South Africa, GeoModel Solar Report 58-01/2011, 2011.
2. *Madaly K and Hoffmann JE*, Identifying the optimum storage capacity of a 100 MW CSP plant in South Africa,

Proceedings of the 2nd South African Solar Energy Conference, Port Elizabeth, 2014.
3. *Turchi CS and Heath GA*, Molten salt power tower cost model for the system advisor model (SAM), National Renewable Energy Laboratory Technical Report NREL/TP-5500-57625, 2013.
4. *Kolb GJ*, An evaluation of possible next-generation high-temperature molten-salt power towers, Sandia Report SAND2011-9320, 2011.
5. *Kost C, Mayer JN, Thomsen J, Hartmann N, Senkpiel C, Philipps S, Nold S, Lude S, Saad N and Schlegl T,* Levelized cost of electricity renewable energy technologies, Fraunhofer Institute for Solar Energy Systems Study, 2013.
6. *Anonymous*, ESKOM Tariffs & Charges Booklet 2012/13.
7. http://www.torresolenergy.com/EPORTAL_DOCS/GENERAL/SENERV2/DOC-cw4cb709fe34477/GEMASOLARPLANT.pdf, 2014.
8. *Duffie JA and Beckman WA*, Solar engineering of thermal processes, 3rd Edition, Wiley, 2006.
9. *Gauché P, Pfenninger S, Meyer AJ, Von Backström TW and Brent AC,* Modelling dispatchability potential of CSP in South Africa, *Proceedings of the 1st South African Solar Energy Conference*, Stellenbosch, 2012.
10. *Anders S, Bialek T, Geier G, Jackson DH, Quintero-Núñez M, Resley R, Rohy DA, Sweedler A, Tanaka S, Winn C and Zeng K,* Potential for renewable energy in the San Diego region, Published by the San Diego Regional Renewable Energy Group, 2005.
11. *Herrmann U and Kearney DW*, Survey of thermal energy storage for parabolic trough power plants, *Journal of Solar Energy Engineering,* 2002, 124(2), 145-152.
12. *Young MF and Ulrich TR*, Mixed convection heat transfer from a vertical heated cylinder in a crossflow, *International Journal of Heat and Mass Transfer,* 1983, 26(12), 1889 – 1983.
13. *Cengel YA and Ghajar AJ*, Heat and mass transfer: Fundamentals and applications, 4th Edition, McGraw-Hill, 2011.
14. *Burger L*, A high resolution model for multiple source dispersion of air pollutants under complex atmospheric structure, PhD Thesis, University of Natal, 1986.
15. *Sioshansi R and Denholm P*, The value of concentrating solar power and thermal energy storage, Technical Report, NREL-TP-6A2-45833, 2010.
16. *Pérez-Segarra, CD, Rodríguez I, Oliva A, Torras S, and Lehmkuhl O,* Detailed numerical model for the resolution of molten salt storage tanks for CSP plants, *Proceedings of 2nd International Conference on Solar Heating, Cooling and Buildings,* Rejika, 2012.
17. *Behbahani-nia A, Sayadi S and M Soleymani, M*, Thermoeconomic optimization of the pinch point and gas-side velocity in heat recovery steam generators, *Journal of Power and Energy*, 2010, 224(6), 761 – 771.
18. *Anonymous*, Steam turbines for CSP plants, www.siemens.com/energy, 2010.
19. *Anonymous*, (s.a), http://xsteam.sourceforge.net/, 2014.
20. *Kearton WJ*, Steam turbine theory and practice, 4th Edition, Sir Isaac Pitman and Sons, London, 1944.
21. *Pretorius JP and Du Preez AF*, Eskom cooling technologies, *Proceedings of the 14th IAHR Conference*, Stellenbosch, 2009.
22. *Söylemez MS*, On the thermo economical optimization of feed water heaters in thermal power plants, *Smart Grid and Renewable Energy*, 2011, 2(4), 410 – 416.
23. Anonymous, http://www.thermoflow.com/convsteamcycle_ STP.html, s.a.
24. *Tyner GE, Sutherland JP and Gould WR*, Solar II: A molten salt power tower demonstration, *VDI-GET Conference: Solar Thermal Power Plants II*, Stuttgart, 1995.
25. *Madaly K*, Identifying the optimum storage capacity for a 100-MW_e concentrating solar power plant in South Africa, M Eng Thesis, Department of Mechanical and Mechatronic Engineering, Stellenbosch University, South Africa, 2014.
26. *Anonymous*, ESKOM Holdings SOC limited Integrated Report – 2014, 2014.
27. http://www.safarmtraders.co.za/farms-for-sale-in-upington-c530, 2014.
28. *Augsburger G*, Thermo-economic optimisation of large solar tower power plants, PhD Thesis, Swiss Federal Institute of Technology, Lausanne, 2013.
29. *Avila-Marin AL, Fernandez-Reche J and Tellez FM*, Evaluation of the potential of central receiver solar plants: configuration, optimization and trends, *Applied Energy*, 2013, 112, 274 – 288.
30. Anonymous, (s.a.), https://sam.nrel.gov, 2014.
31. *Miketa A and Merven B*, Southern African power pool: Planning and prospects for renewable energy, International Renewable Energy Agency Report, 2012.
32. *MacColl B.*, Energy policy – a utility perspective, *South Africa's Electricity Supply Conference*, Johannesburg, 2013.